for $L > 0$. As seen in Figure 7, eq 17 is equivalent to $Q(L) \sim [\exp(-3L^2/2)]/L$, which is eq 2 with $M = 2$, for $L > 0.1$ and levels off for values less than 0.1. Therefore, the partition function is approximated well by using eq 2 for $L > L^*$ and $Q(L) = Q(L^*)$ for $L < L^*$. The results for the junction fluctuations and force are fairly insensitive to the exact value of L^* chosen.

Appendix B: Results for Large M by the Method of Steepest Descents

The mean-square junction fluctuations and the uniaxial force for the micronetwork both can be expressed in terms of the integral

$$l_\alpha^{\,i} = \int_V \mathrm{d}\mathbf{r}\; w_a^{\,i}(r)\; e^{-Mh(r)} \tag{18}$$

where $w_\alpha^{\,i}(r)$ is given by

$$w_\alpha^{\,i}(r) = y_i^{\alpha} \exp[-\beta^2 \sum_1^3 (\mathbf{r}_j - \mathbf{r})^2] \tag{19}$$

From the above, $\langle \delta y_i^2 \rangle = l_2^{\,i}/l_0$ and $f = -\partial \ln l_0/\partial\lambda$.

The integral l_α can be solved by the method of steepest descents for large M.[15] The first step is to find the position of the junction for which $\partial h/\partial y_i$ vanishes. The resulting position is $r^* = (0,-N^{1/2}lk,0)$, where $k(\lambda)$ is given by eq 12. The second step is to calculate the second derivatives of h, $h_{ij} = \partial^2 h/\partial y_i \partial y_j$, evaluated at r^*. The cross terms ($i \neq j$) vanish, and $(Nl^2/9)h_{11} = 1 + s(\lambda)$ and $(Nl^2/9)h_{22} = 1 - s(\lambda)$, where s is given by eq 11. The integrals l_α can then be expressed as

$$l_\alpha^{\,i} = e^{-\beta^2 Mh(r^*)} \int_{-\infty}^{\infty} \mathrm{d}y_i\; y_i^{\alpha} \exp[-\beta^2(3 + \tfrac{1}{2}Mh_{ii})y_i^2] \prod_{j \neq i} \int_{-\infty}^{\infty} \mathrm{d}y_j \exp[-\beta^2(3 + \tfrac{1}{2}Mh_{jj})y_j^2] \tag{20}$$

Evaluating the integrals results in eq 10 for the junction fluctuations and the following for the partition function:

$$-\ln Z \sim \beta^2 Mh(r^*) + \tfrac{1}{2}\sum_1^3 \ln h_{ij} \tag{21}$$

where only the strain-dependent portion of the partition function has been retained.

The uniaxial force is found by differentiating eq 21 with respect to the extension ratio, which results in

$$f = f_F + \frac{1}{2}\sum_1^3 \frac{\partial h_{ii}/\partial\lambda}{h_{ii}} = f_F - \frac{1}{2}\sum_1^3 \frac{\partial \langle \delta y_i^2 \rangle/\partial\lambda}{\langle \delta y_i^2 \rangle} \tag{22}$$

where f_F is the free energy of the network with the junction fixed at its most probable position (from the first term in eq 21). With the "fluctuation volume" defined as $(\langle \delta y_1^2 \rangle \langle \delta y_2^2 \rangle \langle \delta y_3^2 \rangle)^{1/2} \cong \langle \delta y^2 \rangle^{3/2}$ due to the relatively weak strain dependence of the junction fluctuations, the force can be approximately represented by eq 13.

References and Notes

(1) Treloar, L. R. G. *The Physics of Rubber Elasticity*; Oxford University Press: London, 1958.
(2) Flory, P. J. *Principles of Polymer Chemistry*; Cornell University Press: Ithaca, NY, 1956.
(3) James, H. M.; Guth, E. *J. Chem. Phys.* **1943**, *11*, 455.
(4) Ronca, G.; Allegra, G. *J. Chem. Phys.* **1975**, *63*, 4990.
(5) Flory, P. J. *J. Chem. Phys.* **1977**, *66*, 5720.
(6) Marrucci, G. *Macromolecules* **1981**, *14*, 434.
(7) Gaylord, R. J. *Polym. Bull.* **1983**, *9*, 156.
(8) Ball, R. C.; Doi, M.; Edwards, S. F.; Warner, M. *Polymer* **1981**, *22*, 1010.
(9) Adolf, D. *Macromolecules* **1987**, *20*, 116.
(10) Doi, M.; Edwards, S. F. *The Theory of Polymer Dynamics*; Oxford University Press: Oxford, 1986.
(11) Allen, G.; Burgess, J.; Edwards, S. F.; Walsh, D. J. *Proc. R. Soc., London* **1973**, *A334*, 453.
(12) Ronca, G.; Allegra, G. *J. Chem. Phys.* **1975**, *63*, 4104.
(13) Martin, J. E.; Eichinger, B. E. *Macromolecules* **1980**, *13*, 626.
(14) Adolf, D.; Curro, J. G. *Macromolecules* **1987**, *20*, 1646.
(15) Wyld, H. W. *Mathematical Methods for Physics*; Addison-Wesley: Reading, MA, 1979.

Investigation of Relaxation Processes in Low and High Molecular Weight Bulk Poly(methyl methacrylate) by Dynamic Light Scattering

G. Fytas*

Research Center of Crete and Department of Chemistry, University of Crete, Iraklion, Crete, Greece

C. H. Wang

Department of Chemistry, University of Utah, Salt Lake City, Utah 84112

E. W. Fischer

Max Planck Institut fur Polymerforschung, P.O. Box 3148, 6500 Mainz, FRG.

Received July 27, 1987; Revised Manuscript Received January 13, 1988

ABSTRACT: Photon correlation functions of the polarized component of the scattered light from a low molecular weight PMMA (M_w = 3900, T_g = 52 °C) have been studied in the temperature range 65–98 °C. The observed relaxation functions have been represented by a multiexponential decay by using an inverse Laplace transform analysis. The computed spectrum of retardation times reveals a two-peak structure like that observed in the high molecular weight material (T_g = 107 °C). The temperature dependences of the long-time peak associated with the primary glass–rubber relaxation in the two PMMA's are similar when compared at temperatures equidistant from their T_g's. The light scattering and ultrasonic data on the longitudinal density fluctuations over 12 decades in time conform to a single Vogel–Fulcher–Tamman–Hesse equation. The relaxation times of the short-time peak in the retardation spectrum are insensitive to T_g and compare favorably with dielectric data associated with the secondary β-relaxation.

Introduction

Dynamic light scattering has proved to be a potential method for the study of bulk polymer dynamics near and above the glass transition temperature (T_g). The dynamics of the thermodynamic fluctuations in the density and optical anisotropy in the time range 10^{-6}–10^2 s can be

0024-9297/88/2221-2253$01.50/0

© 1988 American Chemical Society

investigated by photon correlation spectroscopy.[1] For weakly anisotropic scatterers, such as the segments of poly(methyl methacrylate), the dominant contribution to the light scattering intensity arises from density fluctuations.

The density time correlation function $c(t)$ which has a highly nonexponential shape is dominated by the so-called primary glass–rubber relaxation for all studied polymers except poly(alkyl methacrylates).[2,3] The mean relaxation time exhibits strong temperature and pressure dependence but is independent of chain length and the probing wavelength.[4] These findings suggest that localized segmental motions of the polymer chain grossly affect the slow density fluctuations in undiluted polymers near T_g. Recently, the $c(t)$ has been related with the time-dependent longitudinal compliance $D(t)$[5,6] which otherwise cannot be easily obtained.

In a recent publication, we have shown that the photon correlation function of high molecular weight poly(methyl methacrylate) (PMMA) consists of two discrete relaxation modes.[7] Between the glass transition temperature (T_g = 380 K) and 422 K, the whole dynamic range encompassing more than seven decades in time is needed in order to obtain a fully relaxed time correlation function $c(t)$. However, due to the presence of a fast mode, the relaxed $c(t)$ could not be obtained at short times (10^{-6} s), even at temperatures near T_g. This limitation may affect the mean relaxation time associated with the fast process obtained by using the inverse Laplace transform of the $c(t)$.

The relaxation time of the fast mode is insensitive to T_g and, hence, insensitive to the polymer molecular weight (MW).[2,7] Using a low MW PMMA sample, we can therefore perform photon correlation measurements at temperatures lower than 380 K and shift the fast mode into the measurable time range of the correlator. At sufficiently low temperatures we expect the relaxation function $c(t)$ when plotted versus log t to reach a plateau value at short times. This will prevent cutoff effects in the Laplace inversion of $c(t)$ and assist the data analysis needed for the high MW PMMA.[7]

In this paper, we have reported the result of studies of the MW effect on the shape of the time correlation function of PMMA, thereby to elucidate the nature of the two relaxation modes using a sufficiently low MW sample (M_w = 3900, M_w/M_n = 2.19 T_g = 52 °C). In addition, the slow relaxation process present in this polydispersed low MW PMMA is expected to exhibit a different temperature dependence than that in the high MW polymer. The MW dependence has also been previously investigated in poly(propylene glycol).[4] However, in that polymer only one relaxation process (i.e., the glass–rubber relaxation) dominates $c(t)$ and in this low MW material the T_g already reaches the asymptotic high MW value.

Experimental Section

The time correlation functions at different temperatures were taken at a scattering angle of 90° following the procedure described elsewhere.[7] The light source was an argon ion laser (Lexel) operating at λ_0 = 514.5 nm with a power of about 400 mW. The single clipped intensity autocorrelation function $G(t)$ over 4.3 decades in time was measured in one run by means of 28 channel Malvern log–lin correlator (K-7027). The desired normalized relaxation function $c(t)$ associated with the density fluctuations is computed from $G(t)$ through the equation

$$G(t) = A[1 + b|c(t)|^2] \quad (1)$$

where A is the base line computed or measured at long delay times t and the amplitude b is considered as a fitting parameter. Below

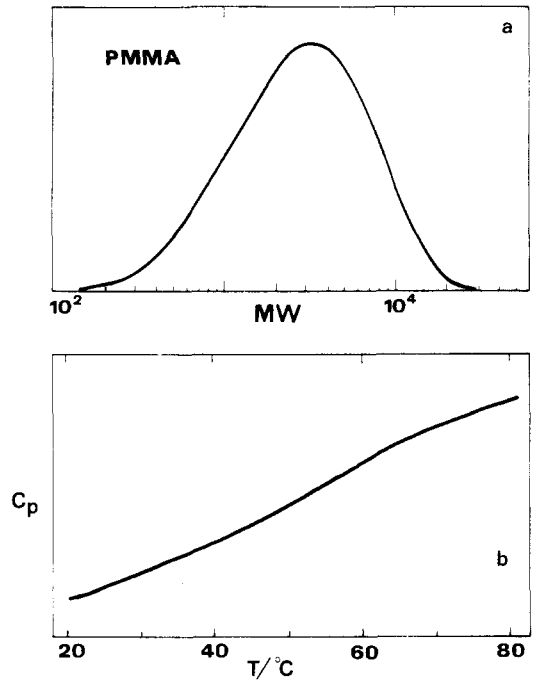

Figure 1. (a) Gel permeation chromatography curve of low molecular weight poly(methyl methacrylate). (b) Heat capacity of amorphous PMMA obtained by differential scanning calorimetry with a heating rate of 10 °C/min plotted versus temperature.

80 °C a time range larger than 4.3 decades is required to obtain $G(t)$. To encompass a larger dynamic range, two or three partially overlapping correlation functions measured in separate runs with different sample times were spliced together by using the procedure described elsewhere.[4]

Unlike the situation in high MW PMMA, where a significant amount of the scattering intensity is still present beyond 10^{-6} s, the relaxation functions $c(t)$ for the low MW PMMA at temperatures below 80 °C tends to asymptotically reach a plateau value, using the shortest delay time of the correlator. Hence the intercept b can reliably be obtained in this case.

The low MW sample was kindly provided by Dr. W. Wunderlich, of Röhm (Darmstadt), West Germany. Gel permeation chromatography (GPC) yielded a number-average MW (M_n) of 1800 and a weight-average MW (M_w) of 3900. The GPC curve is shown in Figure 1a. The glass temperature (T_g) was determined with a differential scanning calorimeter. The inflection point occurs at T_g = 52 °C for a heating rate of 10 K/min; see Figure 1b. It is worth noting that the width ΔT of the transition is relatively broad (~40 K). This probably reflects polydispersity effects in the low MW polymer.

To prepare a good undiluted polymer sample, the PMMA was first dissolved in benzene and then filtered through a 0.22-μm Millipore filter into the dust-free light scattering cell. After freeze-drying to remove the solvent and heating at about 180 °C in a vacuum oven the sample was then annealed above T_g for several days to obtain an optically clear homogeneous and strain-free probe suitable for photon correlation measurements.

Data Analysis. The net experimental correlation function $(G(t)/A - 1)^{1/2}$ with fixed measured base line was used to process the data. First, we used the Kohlrausch–Williams–Watts (KWW) fractional exponential decay[4]

$$(G(t)/A - 1)^{1/2} = b^{1/2} \exp[-(t/\tau_0)^{\beta}] \quad (0 < \beta \leq 1) \quad (2)$$

to represent the experimental correlation functions treating b and τ_0 as adjustable parameters. The distribution parameter was found to change from 0.26 at 98 °C to 0.16 at 65 °C in contrast to the usual situation of nearly constant β (about 0.35) reported for most bulk polymers.[1] This behavior is similar to that observed in others poly(alkyl methacrylates)[2,3,8,9] and was interpreted to be due to the overlap of two relaxation processes. The normalized correlation functions $|c(t)|^2$ are plotted versus log t in Figure 2.

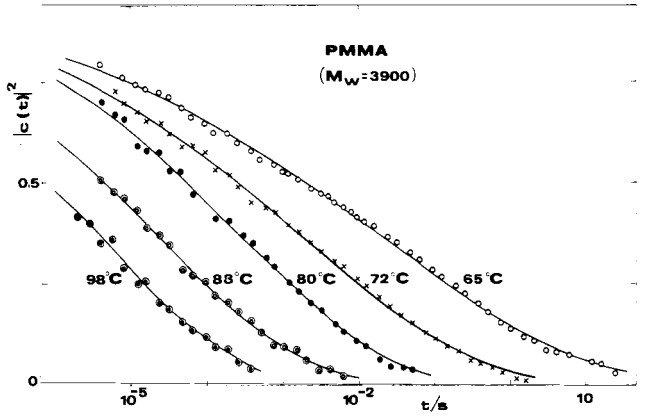

Figure 2. Measured normalized homodyne photon correlation functions ($|c(t)|^2 = [G(t) - A]/Ab$) at four temperatures of bulk low MW PMMA (T_g = 52 °C). The 72 and 65 °C data are composite correlation functions.

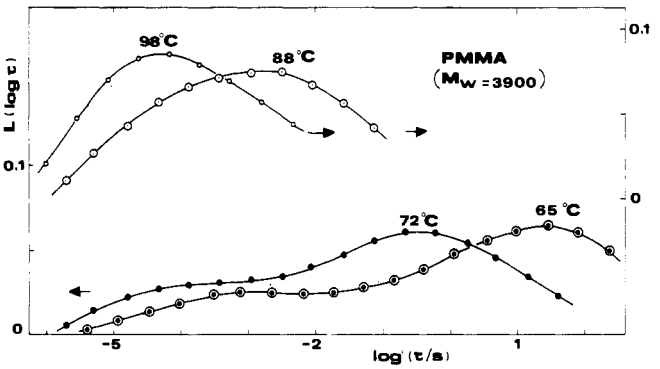

Figure 3. Retardation time spectra $L(\log \tau)$ plotted versus log τ for low MW PMMA (T_g = 52 °C) at four temperatures obtained from the inverse Laplace transform analysis of the time correlation functions.

A systematic deviation from the single KWW fit of eq 2 is evident at low temperatures.

A more appropriate data analysis was recently undertaken for high MW PMMA.[7] By use of a modified computer program originally developed by Provencer,[10] the continuous spectrum of retardation times $L(\ln \tau)$ can be extracted from the correlation functions.

$$b^{1/2}c(t) = \int_{-\infty}^{\infty} L(\ln \tau)e^{-t/\tau}\, d \ln \tau \qquad (3)$$

Figure 3 shows the results of the inverse Laplace transform (ILT) analysis of the experimental correlation functions of PMMA at four temperatures above T_g. As expected the temperature-dependent β-parameter gives rise to the significant change in the shape of the $L(\log \tau)$ as the temperature decreases toward T_g. This method of analysis does not require an a priori assumption of the form of the $c(t)$.

Results and Discussion

Primary Glass–Rubber Relaxation (Slow Process). Unlike the situation in high MW PMMA,[7] there is strong evidence that the correlation functions obtained from the low MW sample (Figure 2) reach asymptotically a short time plateau value below 80 °C. This makes reliable the determination of b and hence enables the ILT analysis. Up to about 80 °C the ILT analysis shows two broad peaks whereas the corresponding correlation functions exhibit no clear kink similar to that observed in the high MW PMMA.[7] At high temperatures the values of the relaxation time of the slow process are close to that of the relaxation time of the fast mode; as a result the $L(\log \tau)$ displays one broad peak (Figure 3). Using $L(\log \tau)$ to describe the

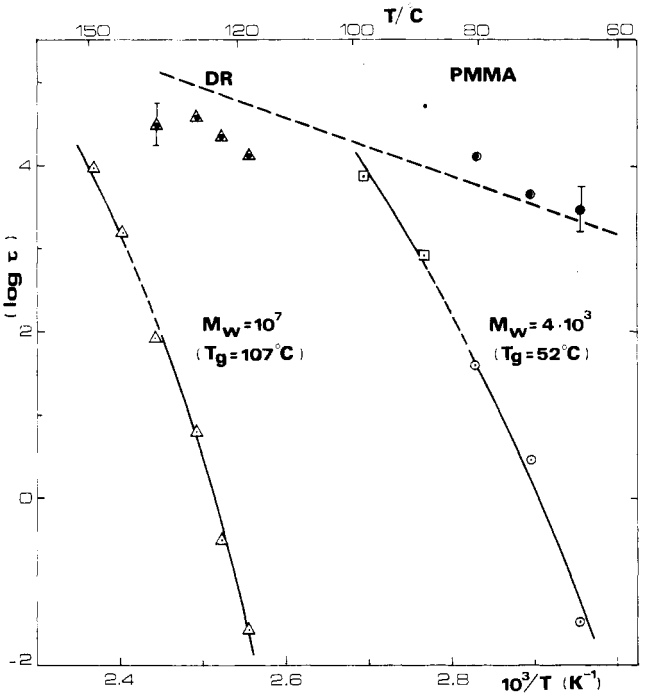

Figure 4. Temperature dependence of the average time $\langle \log \tau \rangle$ of the slow relaxation process (○, □ △) fast relaxation process (●, ▲) and the dielectric β-relaxation time (DR, dashed line) for low and high MW PMMAs.

distribution of retardation times, we write the average value, $\langle \log \tau \rangle$ as the first moment of the $L(\log \tau)$.

$$\langle \log \tau \rangle = \int_{-\infty}^{\infty} \log \tau\, L(\log \tau)\, d \log \tau \Big/ \int_{-\infty}^{\infty} L(\log \tau)\, d \log \tau \qquad (4)$$

Figure 4 shows the temperature dependence of the average $\langle \log \tau \rangle$. The slow relaxation process exhibits a strong variation with temperature and is therefore associated with the primary glass–rubber relaxation. Accordingly, we have fitted the $\langle \log \tau \rangle$ values to the Vogel–Fulcher–Tamman–Hesse (VFTH) equation[11]

$$\langle \log \tau \rangle = \langle \log \tau \rangle_0 + B/(T - T_0) \qquad (5)$$

In the VFTH equation, which is an alternative form of the WLF equation, $\langle \log \tau \rangle_0$, $B = 2.303C_1C_2$, and $T_0 = T_g - C_2$ are characterizing parameters where C_1 and C_2 are the WLF coefficients.

To determine these parameters by using the data obtained over a fairly narrow temperature range, we have used a fixed C_2 = 50 K, deduced from the compliance data obtained for the high MW PMMA sample over a larger temperature range.[11,12] Using this value for C_2 and T_g = 52 °C we obtain $\langle \log \tau \rangle_0 = -14.1$ (τ in s), $B = 2245 \pm 230$ K, and $C_1 = 19.5 \pm 2$. The literature values of the WLF parameter C_1 obtained from the mechanical data of atactic high MW PMMA are not consistent. They range between 32 and 15.[11-13] However, recent photon correlation studies of high MW PMMA have yielded a C_1 value very close to that of the low MW PMMA.[3,7]

The relaxation times of the slow mode for the high MW PMMA[7] are also plotted in Figure 4 for comparison. The temperature dependence as described by the VFTH equation gives the characterizing parameters $\langle \log \tau \rangle_0 = -14.9$ (τ in s), B = 2330 K, and C_1 = 20.2. Closeness of these values to those of the low MW PMMA indicates that the temperature dependences of the two PMMA materials are almost indistinguishable when compared at temperatures equidistant from their T_g's. This situation is clearly

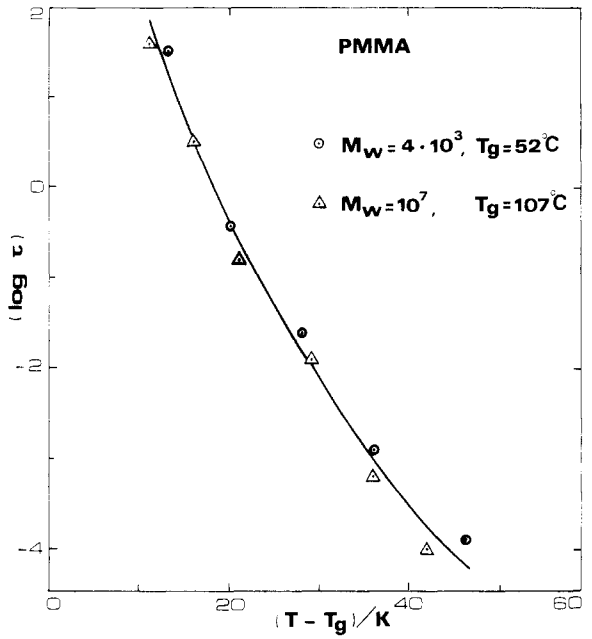

Figure 5. Relaxation time of the slow process for the low (○) and high (△) MW PMMA plotted versus $(T - T_g)$.

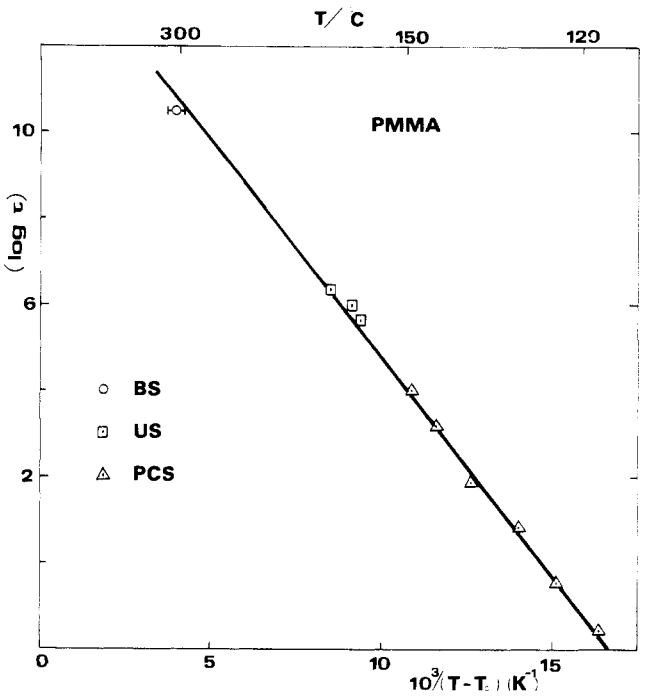

Figure 6. Comparison of the relaxation times of the slow relaxation process obtained from photon correlation (PCS) ultrasonic (US) and Brillouin scattering (BS) for high MW PMMA. The solid line denotes the fit of the experimental times to the VFTH equation.

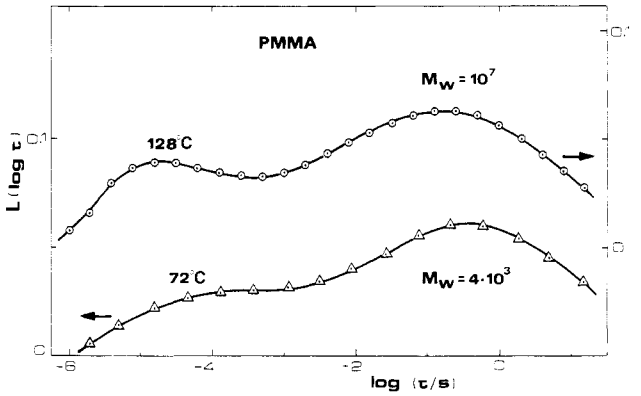

Figure 7. Comparison of the retardation time spectra $L(\log \tau)$ versus $\log \tau$ for the high MW (T_g = 107 °C)[7] at 128 °C and low MW PMMA (T_g = 52 °C) at 72 °C obtained from the inversion of the time correlation functions by using the ILT technique.

shown in Figure 5, where both sets of the slow times $\langle \log \tau \rangle$ fall on a single curve.

The parameter B in eq 5 has so far been viewed through two apparently different theoretical approaches. In the simple three-state rotational isomerization model,[14] B is related to the activation energy of the rotation about the main-chain bonds, with $E_0 = RB$ (R being the gas constant), which incorporates the interaction of the polymer segments. The energy E_0 amounts to 4.5 kcal/mol, which is somewhat higher than the value for poly(methyl acrylate).[15] In the free volume model, B is related to the free volume expansion coefficient $a_f = \gamma/B \simeq 4.4 \times 10^{-4}$ K^{-1} (γ is a constant nearly equal to 1).[11] It seems reasonable to assume that either E_0 or a_f takes similar values in both kinds of PMMA's. Only the value of T_g (and hence T_0) depends on the molecular weight because its reciprocal is proportional to the number of chain ends.[16]

It is useful to compare the photon correlation data with existing mechanical relaxation data for PMMA above T_g. The density correlation function $c(t)$ in eq 1 has recently been shown to be associated with the time-dependent longitudinal compliance $D(t)$ which is otherwise difficult to obtain mechanically.[5] In practice, it is usually the shear modulus (or compliance) or Young's modulus that is measured mechanically. For PMMA, however, the relaxation of the longitudinal modulus M^* ($=1/D^*$) has been investigated by using ultrasonic[17] and Brillouin scattering[18] techniques. The time $1/\omega$ (ω being the sound frequency) for the temperature T_{max} at which the sound attenuation has its maximum value is plotted in Figure 6. The value of T_{max} for the hypersonic absorption obtained from the Brillouin spectrum is a crude estimate.[18] Nevertheless, the three sets of data covering 12 decades in time in the temperature range T_g to $T_g + 200$ can be well represented by the VFTH using C_2 = 50 K. The values of the parameters in eq 5 are similar to those obtained from the fit of the slow relaxation times. Differences between the relaxation time associated with M and the retardation time with D as well as those results under isothermal (photon correlation) and adiabatic (Brillouin) conditions are probably suppressed in the semilog plot of Figure 6.

Secondary Relaxation (Fast Process). The inverse Laplace transform analysis can better reveal the double-relaxation feature of the density correlation function $c(t)$. Below 88 °C the $L(\log \tau)$ function displays two peaks with vastly different temperature dependences. Two relaxation processes were also resolved in the photon correlation functions of the high MW PMMA below 136 °C.[7] Figure 7 shows the $L(\log \tau)$ spectra for the high and low MW PMMA respectively at 128 °C and 72 °C, which are about 20 K higher than T_g. The long-time peaks are associated with the primary glass–rubber relaxation and appear at about the same position (~0.6 s) for both PMMA's. In addition, the shape of $L(\log \tau)$ is similar for the two materials, although the separation between the peaks is larger for the high MW PMMA. These results are consistent with the distinct kink observed in the time correlation function of the high MW PMMA below 128 °C and the presence of a significant scattering intensity at times shorter than 10^{-6} s.[7] In contrast, the time correlation function of the low MW material exhibits no clear kink and it tentatively reaches a short-time plateau below 80 °C (Figure 2).

The average $\langle \log \tau \rangle$ for the fast relaxation process, as shown in Figure 4, is rather insensitive to T_g variation and is less sensitive to temperature variation than the relaxation time of the slow mode, in agreement with dielectric and mechanical relaxation findings.[11,19] An Arrhenius temperature dependence is therefore more appropriate than the free volume equation, (5). Moreover, the presence of the fast mode in PMMA is consistent with the dielectric relaxation process assigned to the hindered rotation of the $COOCH_3$ side group around the C–C bond linking it to the main chain.[19] The dielectric relaxation time $1/(2\pi f_m)$, where f_m is the frequency at the loss permitivity maximum in the high MW PMMA[19] is also plotted in Figure 4 for comparison. Within experimental uncertainty the temperature dependence of the fast light scattering time is compatible with that obtained in the dielectric relaxation. For the latter, the reported Arrhenius activation energy E is 18 kcal/mol.[19] However, we still need to explain why the relaxation times measured in the high MW PMMA at high temperatures exceed the values obtained from the extrapolation of the low MW data by using E = 18 kcal/mol. We attribute this discrepancy to the cutoff effects present in the ILT analysis. This is probably due to the lack of the short-time plateau in the time correlation functions of high MW PMMA.[7] As a matter of fact, to ascertain the influence of the cutoff effect is one of the reasons for initiating the present investigation.

Conclusion

In this work, we present further convincing evidence for the presence of two relaxation modes in the time correlation functions of PMMA near and above T_g. The retardation spectrum obtained by using the inverse Laplace transform analysis reveals a two-peak structure, although the corresponding time correlation function for the low MW sample (T_g = 52 °C) does not show a clear kink like that observed in the high MW material (T_g = 107 °C) below 128 °C. The long-time peak associated with the primary glass–rubber relaxation displays a strong temperature dependence and the relaxation time versus temperature data are well represented by the VFTH free volume equation. Values of various characterizing parameters are similar in the two PMMA's when allowance is made to take into account the difference in T_g. The light scattering and ultrasonic data on the longitudinal density fluctuations over 12 decades in time can also be fitted to the VFTH equation.

The short-time peak in the retardation spectrum, $L(\log \tau)$ is insensitive to T_g and also displays weaker temperature dependence than the long-time peak. The relaxation times of the short-time peak compare favorably with dielectric data associated with the secondary β-relaxation. In the dynamic range of the currently available correlator, the two relaxation processes are better resolved in the high MW PMMA.

Registry No. PMMA, 9011-14-7.

References and Notes

(1) See, for example: Patterson, G. D. *Adv. Polym. Sci.* **1983**, *48*, 125. Fytas, G.; Wang, C. H.; Meier, G.; Fischer, E. W. *Macromolecules* **1985**, *18*, 1492.
(2) Fytas G. In *Physical Optics of Dynamics Phenomena and Processes in Macromolecular Systems* Sedlacek, B., Ed.; W. de Gruyter: Berlin, New York, 1985; p 205.
(3) Patterson, G. D.; Carroll, D. J.; Stevens, J. R. *J. Polym. Sci., Polym. Phys. Ed.* **1983**, *17*, 613.
(4) Wang, C. H.; Fytas, G.; Lilge, D.; Dorfmüller, Th. *Macromolecules* **1981**, *14*, 1363.
(5) Wang, C. H.; Fischer, E. W. *J. Chem. Phys.* **1985**, *82*, 632.
(6) Wang, C. H.; Fytas, G.; Fisher, E. W. *J. Chem. Phys.* **1985**, *82*, 4332.
(7) Fytas, G.; Wang, C. H.; Fisher, E. W.; Mehler, K. *J. Polym. Sci., Polym. Phys. Ed.* **1986**, *24*, 1859.
(8) Meier, G.; Fytas, G.; Dorfmüller, Th. *Macromolecules* **1984**, *17*, 957.
(9) Lee, M.; Ferguson, R.; Jamieson, A. M.; Simha, R.; Cowie, J. M. G. *Polym. Commun.* **1985**, *26*, 66.
(10) Provencer, S. W. *Comput. Phys. Commun.* **1982**, *27*, 213, 229.
(11) Ferry, J. D. *Viscoelastic Properties of Polymers*; Wiley: New York, 1980.
(12) Koppelmann, J. In *Physics of Noncrystalline Solids*; Prins, J. A., Ed.; North Holland: Amsterdam, 1965; p 255.
(13) Plazek, D. J.; Tan, V.; O'Rourke, V. M. *Rheol. Acta* **1974**, *13*, 367.
(14) Miller, A. *Macromolecules* **1978**, *11*, 859.
(15) Fytas, G.; Patkowski, A.; Meier, G.; Dorfmüller, Th. *J. Chem. Phys.* **1984**, *80*, 2214.
(16) Couchman, P. R. *J. Appl. Phys.* **1979**, *50*, 6043.
(17) Kono, R. *J. Phys. Soc. Jpn.* **1960**, *15*, 718.
(18) Li, B. Y.; Jiang, D. Z.; Fytas, G.; Wang, C. H. *Macromolecules* **1986**, *19*, 778.
(19) Tetsutani, T.; Kakizaki, M.; Hideshima, T. *Polym. J.* **1982**, *14*, 305.

Relaxation Times of Polymer Solutions in the Semidilute Region for Zero-Shear Viscosity

Yoshiaki Takahashi,* Masanari Umeda,† and Ichiro Noda

Department of Synthetic Chemistry, Nagoya University, Furo-cho, Chikusa-ku, Nagoya 464, Japan. *Received June 30, 1987; Revised Manuscript Received January 15, 1988*

ABSTRACT: Relaxation times τ_w and τ_0 of polymer solutions in the semidilute region for the zero-shear viscosity $\eta°$ were studied in good and Θ solvents. Here, τ_w is the weight-average relaxation time evaluated from the product of $\eta°$ and the steady-state compliance J_e, and τ_0 is the relaxation time specifying shear rate dependence of viscosity. It is found that τ_0 is proportional to τ_w regardless of concentration and solvent power, and the concentration and molecular weight dependences of both relaxation times can be well understood if the semidilute region for $\eta°$ is divided into two regions, i.e., the dilute and entangled regions for J_e.

Introduction

In previous papers[1,2] we studied viscoelastic properties of linear polymer solutions over a wide range of concentration and presented molecular weight–concentration diagrams for the viscosity at zero-shear rate or the zero-shear viscosity $\eta°$ and for the steady-state compliance J_e, representing energy dissipation and storage processes, respectively. The concentration dependence of $\eta°$ of polymer solutions can be well understood if we take account of semidilute solutions and classify the polymer

†Present address: Tokai Rubber Industries Ltd., 3600 Utazu, Kitatoyama, Komaki 485, Japan.

0024-9297/88/2221-2257$01.50/0 © 1988 American Chemical Society